Effect of Alloying Elements on the Corrosion Behavior of Carbon Steel in CO_2 Environments

Yoon-Seok Choi,[‡,] Srdjan Nešić,[*] and Hwan-Gyo Jung[**]*

ABSTRACT

The objective of the present study was to evaluate the effect of alloying elements (Cr, Mo, and Cu) on the corrosion behavior of low carbon steel in CO_2 environments. Six samples were prepared with varying Cr content from 0 wt% to 2 wt% and with added 0.5 wt% of Mo and Cu; the specimens had ferritic/pearlitic microstructures. Steel samples were exposed to a CO_2-saturated 1 wt% NaCl solution with different combinations of pH and temperature (pH 4.0 at 25°C, pH 6.6 at 80°C, and pH 5.9 at 70°C). Changes in corrosion rate with time were determined by linear polarization resistance measurements. The surface morphology and the composition of the corrosion product layers were analyzed by surface analysis techniques (scanning electron microscopy and energy dispersive x-ray spectroscopy). Results showed that the presence of Cr and Cu showed a slight positive effect on the corrosion resistance at pH 4.0 and 25°C. At pH 6.6 and 80°C, regardless of the alloying elements, the trend of corrosion rate with time was similar, i.e., the corrosion rate of all specimens decreased with time resulting from the formation of protective $FeCO_3$. A beneficial effect of Cr presence was clearly seen at "gray zone" conditions: pH 5.9 and 70°C, where steel sample without Cr showed no decrease in corrosion rate with time. The presence of Cr in the steel promoted the formation of protective $FeCO_3$ with Cr enrichment and it decreased the corrosion rate.

KEY WORDS: alloying element, CO_2 corrosion, $FeCO_3$, low Cr steel

INTRODUCTION

Internal environment encountered in the oil and gas transportation pipelines can cause severe corrosion of mild steel mainly resulting from the presence of CO_2, H_2S, organic acids, and water. In CO_2 environments, low carbon steel has often been used in combination with corrosion inhibitor because it is considered the most cost effective option, compared with utilizing expensive corrosion resistant alloys.[1] The corrosion protection of low carbon steel depends on either the spontaneous formation of protective corrosion product layers which is influenced by environmental parameters (CO_2 content, solution chemistry, pH, temperature, fluid velocity, etc.) and material parameters (microstructure and chemical composition)[2] or the addition of corrosion inhibitors. To date, many studies[3-8] have been conducted to understand the effect of both the environmental and metallurgical conditions on corrosion behavior of steels in CO_2 environments.

In recent years, there has been an attempt to use low-Cr alloy steel (0.5% ~ 3% Cr) in CO_2 environments without inhibitor injection because adding Cr to low alloy steel could enhance corrosion resistance at high temperatures and high pressures.[9-10] It has been reported that the addition of Cr contributes to the enrichment of Cr in the corrosion products, which causes the corrosion product layers to be more protective. In addition, an increase in Cr content could lower both the uniform corrosion rate and susceptibility to localized corrosion in CO_2 environments.[11-16]

Although it is evident that small contents of Cr in low alloy steel decrease the corrosion attack, most of the

Submitted for publication: October 30, 2017. Revised and accepted: December 25, 2017. Preprint available online: December 25, 2018, https://doi.org/10.5006/2705.

[‡] Corresponding author. E-mail: choiy@ohio.edu.
[*] Institute for Corrosion and Multiphase Technology, Department of Chemical and Biomolecular Engineering, Ohio University, Athens, OH 45701.
[**] Technical Research Lab., POSCO, Pohang, South Korea.

ISSN 0010-9312 (print), 1938-159X (online)
18/000093/$5.00+$0.50/0 © 2018, NACE International

research studies have focused on the corrosion behavior in very specific ranges of environmental parameters, such as pH, temperature, CO_2 content, etc.[17] Thus, it is necessary to evaluate the effect of Cr presence on the corrosion behavior of low alloy steel under various scenarios encountered in the internal environments for the oil and gas transport pipelines. The objective of the present study was to evaluate the effect of Cr on the corrosion behavior of low alloy steel under different combinations of pH and temperature. Those combinations result in widely differing conditions with respect to whether protective corrosion product layers would form. The effect of minor additions of Mo and Cu on the corrosion behavior was also investigated.

EXPERIMENTAL PROCEDURES

The test specimens with different alloying elements were prepared using the vacuum arc melting furnace and a pilot plant rolling machine. To rule out microstructural effects, the rolling and cooling process were restricted by high-temperature rolling (>850°C) and air-cooling. Total reduction of finish rolling was 75%. All materials were analyzed for chemical composition using atomic emission spectroscopy. Table 1 shows chemical compositions of the six steels used in the present study.

The specimens for the corrosion test were machined with two different geometries: cylindrical type with 5 cm^2 exposed area for electrochemical measurements, and rectangular type with a size of 1.27 cm × 1.27 cm × 0.254 cm for surface analysis. The specimens were sequentially ground with 250, 400, and then 600 grit silicon carbide (SiC) paper, cleaned with isopropyl alcohol in an ultrasonic bath, and dried.

An aqueous electrolyte was prepared from deionized water with 1 wt% NaCl. The solution was initially deoxygenated by bubbling CO_2. This procedure assured that the dissolved oxygen levels were kept below 20 ppb. The pH of the solution was adjusted by adding either deoxygenated acid (HCl) or base ($NaHCO_3$) in sufficient quantity to reach the desired pH. Corrosion tests were performed in a 2 L glass cell under atmospheric pressure. The setup consisted of a: (1) three-electrode corrosion cell (counter electrode: platinum wire, reference electrode: Ag/AgCl electrode); (2) hot plate equipped with temperature controller; (3) CO_2 gas supply set; (4) condenser; (5) potentiostat; and (6) pH meter.

TABLE 2
Test Conditions for Corrosion Testing

Condition	pCO_2 (bar)	Temperature (°C)	pH	Solution
$FeCO_3$-free	0.97	25	4	1 wt% NaCl (stagnant)
$FeCO_3$-forming	0.52	80	6.6	1 wt% NaCl (stagnant)
In between	0.68	70	5.9	1 wt% NaCl (stagnant)

The corrosion properties of carbon steels were evaluated by electrochemical techniques (open-circuit potential [OCP], linear polarization resistance [LPR], and potentiodynamic polarization measurements), and surface analytical techniques (scanning electron microscopy [SEM] and energy dispersive x-ray spectroscopy [EDS]). LPR measurements were performed within ±10 mV with respect to the corrosion potential with a scan rate of 0.166 mV/s. The potentiodynamic polarization tests were performed after conducting LPR measurements. The specimen was scanned potentiodynamically at a rate of 0.166 mV/s from the OCP to –1.0 V vs. saturated Ag/AgCl. Then the scan was performed in the anodic direction from OCP to –0.45 V vs. saturated Ag/AgCl, with a scan rate of 0.166 mV/s. After the experiment, the specimen was used for additional ex situ analyses. The morphology and compositions of corrosion products were analyzed by using SEM and EDS.

Table 2 lists the key test conditions for the present study. The test conditions were set in order to investigate the effect of alloying elements for different scenarios common in CO_2 corrosion of mild steel, some of which would include formation of protective $FeCO_3$ corrosion product layers (at high temperature, 80°C) and others would not (at room temperature, 25°C), with conditions at 70°C being in between.

RESULTS AND DISCUSSION

Figure 1 shows the microstructure of low carbon steels with different alloying elements. It was taken at quarter position through thickness in transverse direction. The basic microstructure of all samples was ferrite and pearlite mixture. Although the manufacturing process parameters were all the same, the

TABLE 1
Chemical Compositions of Materials Used in the Present Study (wt%, balance Fe)

No.	C	Mn	Si	P	S	Al	Cr	Ni	Mo	Cu
1	0.041	1.39	0.278	0.008	<0.003	0.028	–	0.287	–	–
2	0.038	1.43	0.266	0.009	<0.003	0.019	0.519	0.307	–	–
3	0.043	1.45	0.248	0.009	<0.003	0.023	1.000	0.292	–	–
4	0.042	1.40	0.254	0.008	<0.003	0.022	1.890	0.308	–	–
5	0.040	1.41	0.248	0.008	<0.003	0.024	0.520	0.309	0.53	–
6	0.040	1.38	0.248	0.008	<0.003	0.024	0.497	0.307	–	0.50

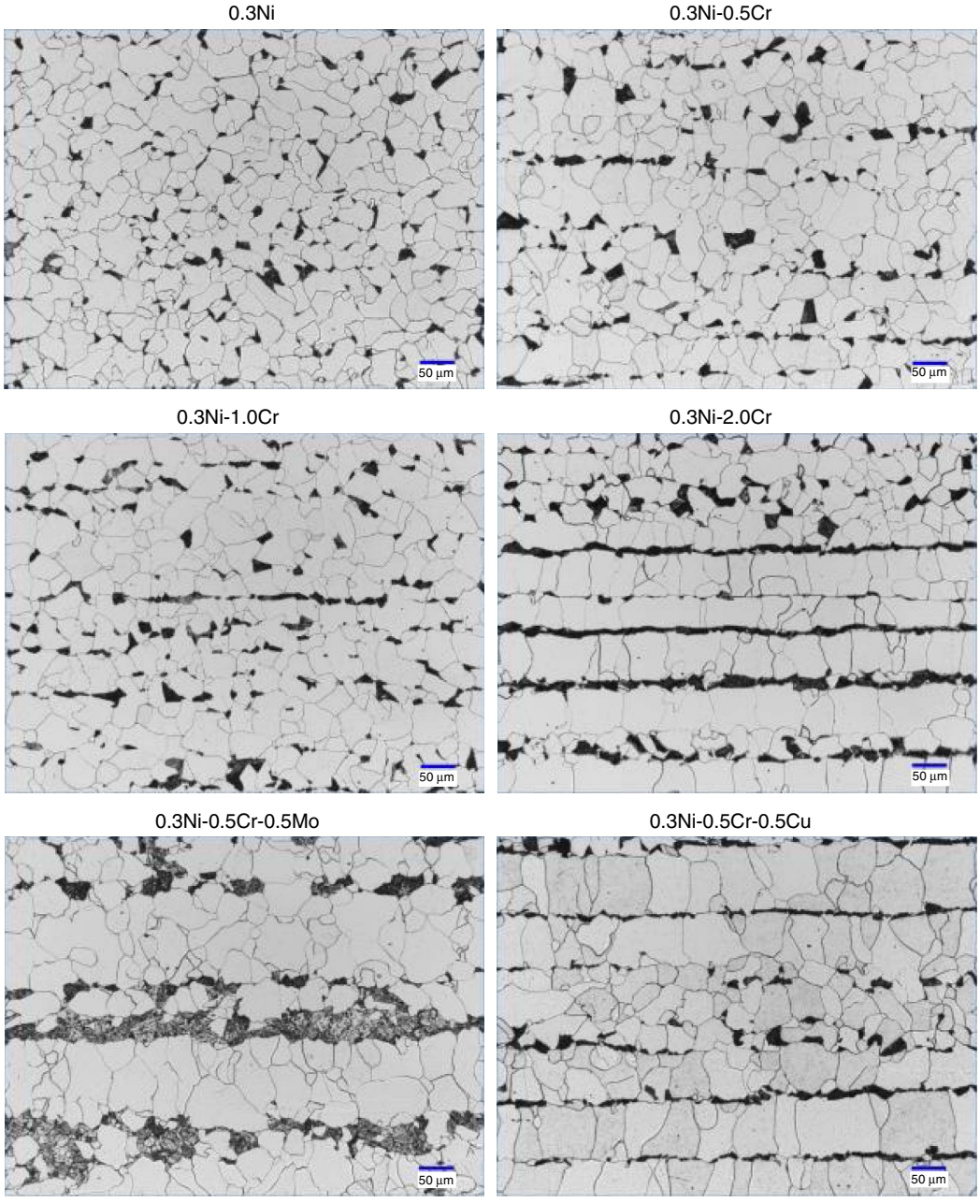

FIGURE 1. *Optical image of the microstructure for different carbon steels (×200, 2% Nital).*

microstructures such as grain size, band structure, and pearlite portion are slightly different because of the alloying elements. The pearlite portion was increased from 7% to 15% with increasing Cr content. Furthermore, the additions of Cr and Mo increased the grain size of ferrite.

Experiments at pH 4 and 25°C

For these conditions where the formation of protective $FeCO_3$ corrosion product layers was not expected, the results of LPR corrosion rate measurements for different carbon steels are described in Figure 2. The polarization resistance values obtained from LPR were converted to corrosion rates with B value of 26 mV. The alloyed steels exhibited more resistance to corrosion than 0.3Ni steel. The results indicate that the presence of Cr slightly decreases the corrosion rate, while additional Cr content has minimal impact. Furthermore, presence of Mo did not change the corrosion rate, but the corrosion rate was slightly reduced by adding Cu.

Figure 3 illustrates the polarization curves for different carbon steels at pH 4 and 25°C. As shown in Figure 3(a), with increasing Cr content, both

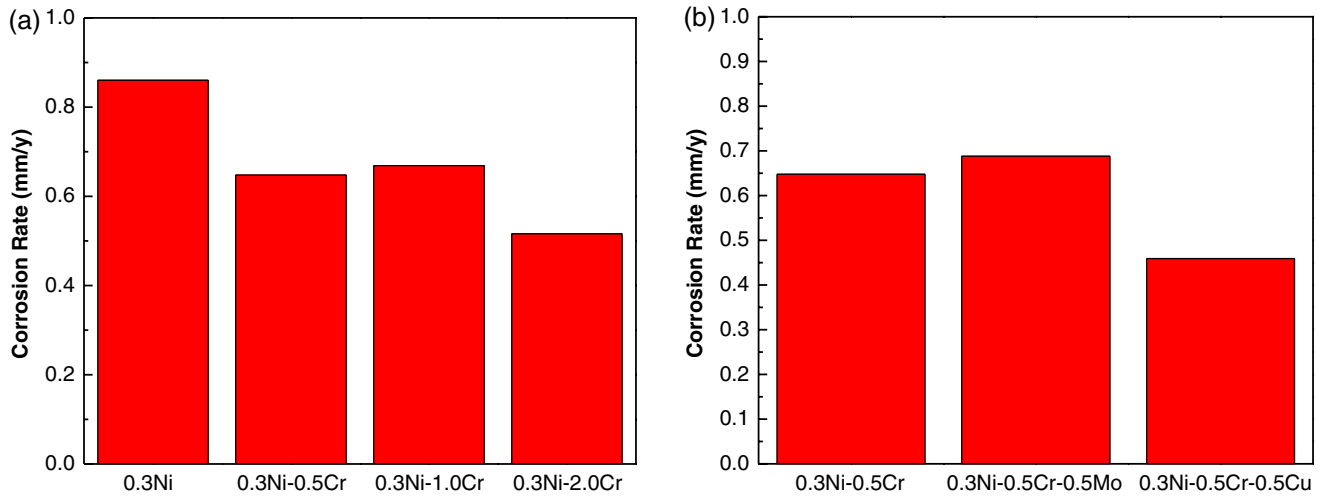

FIGURE 2. *Effect of alloying elements on the corrosion rate in 1 wt% NaCl solution at pH 4 and 25°C: (a) Cr effect and (b) Mo and Cu effect.*

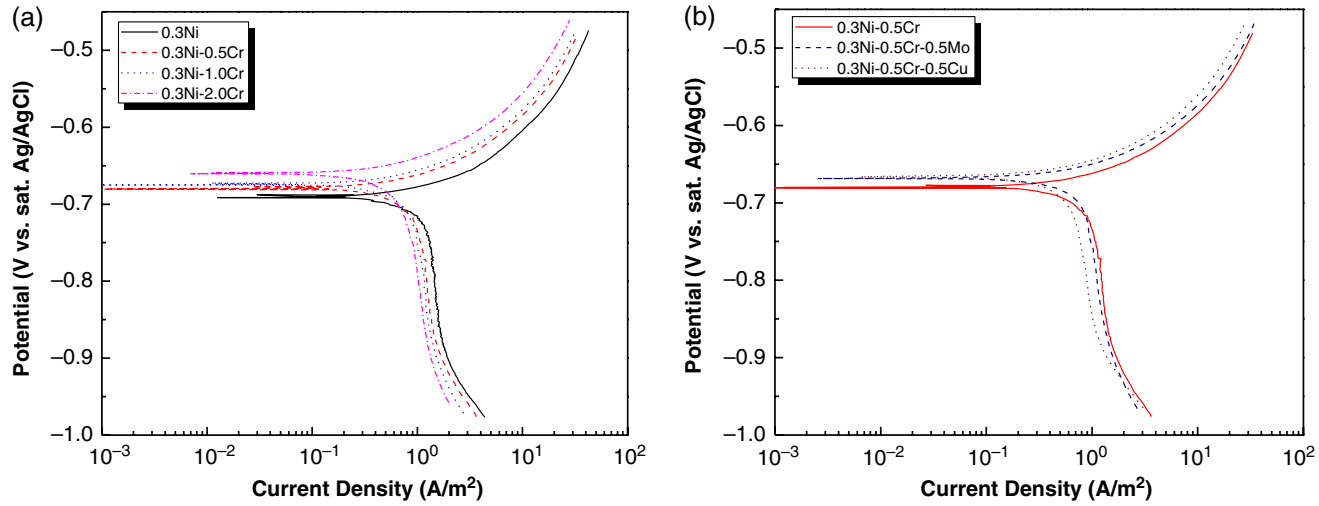

FIGURE 3. *Polarization curves of different carbon steels at pH 4 and 25°C: (a) Cr effect and (b) Mo and Cu effect.*

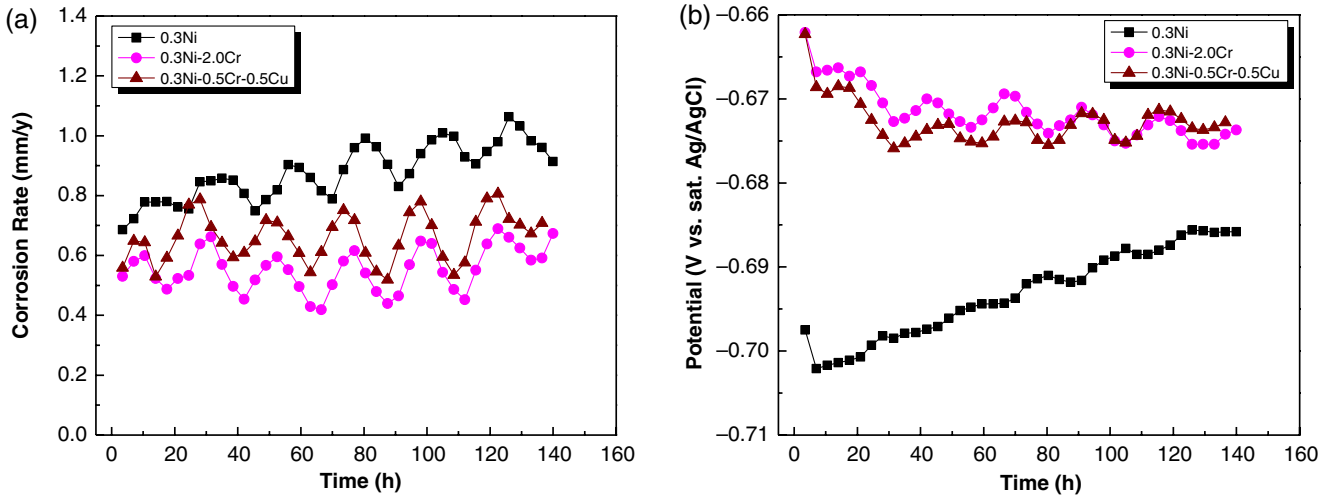

FIGURE 4. *Variations of (a) corrosion rate and (b) corrosion potential for carbon steels with different alloying elements at pH 4 and 25°C.*

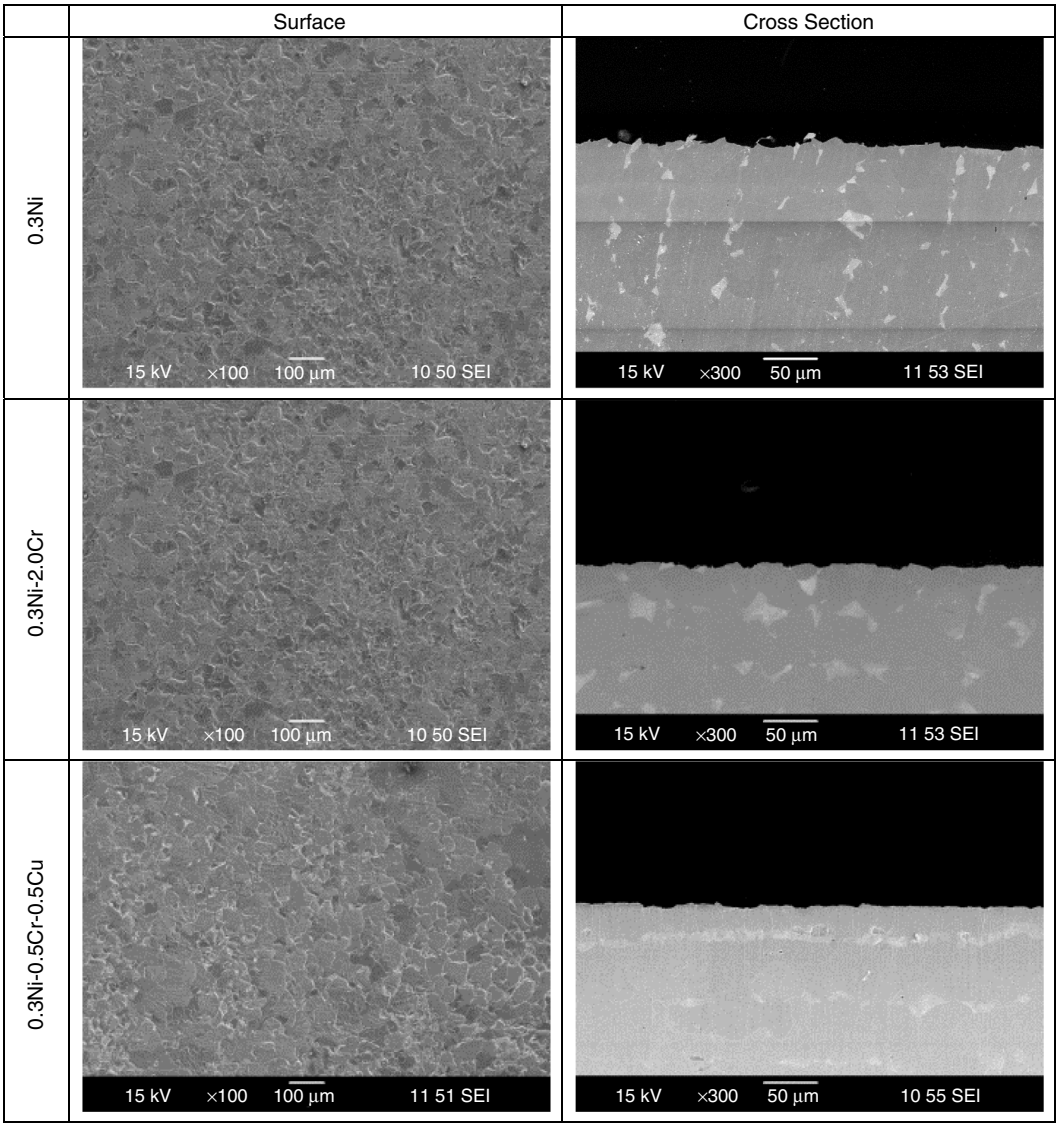

FIGURE 5. *SEM surface and cross-section images of the corroded samples exposed to 1 wt% NaCl at pH 4 and 25°C.*

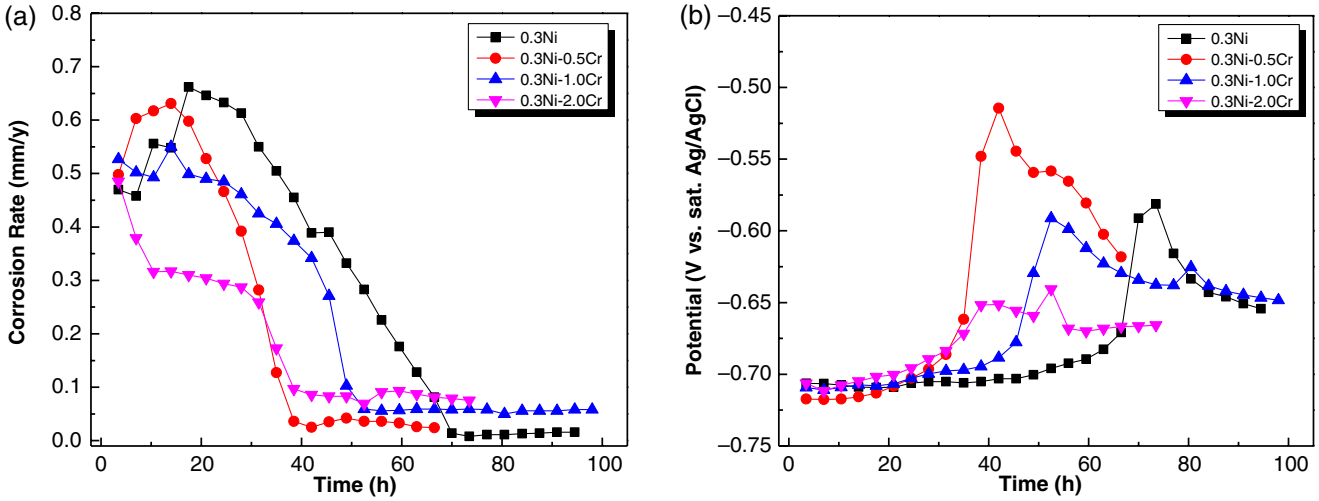

FIGURE 6. *Variations of (a) corrosion rate and (b) corrosion potential for carbon steels with different Cr contents at pH 6.6 and 80°C.*

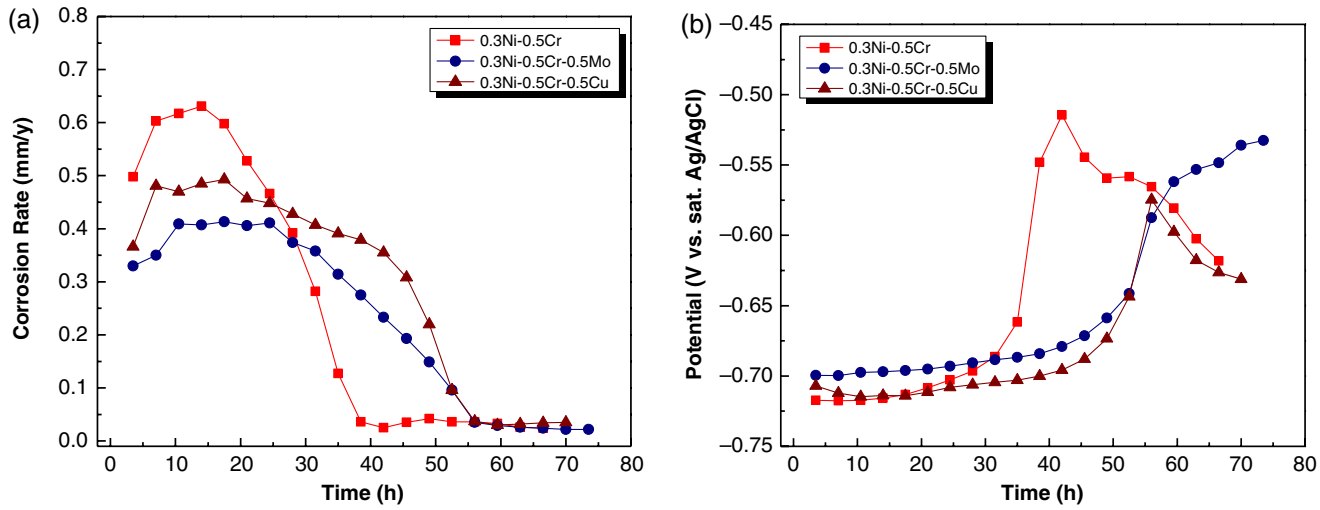

FIGURE 7. *Variations of (a) corrosion rate and (b) corrosion potential for carbon steels with different alloy elements (Mo and Cu) at pH 6.6 and 80°C.*

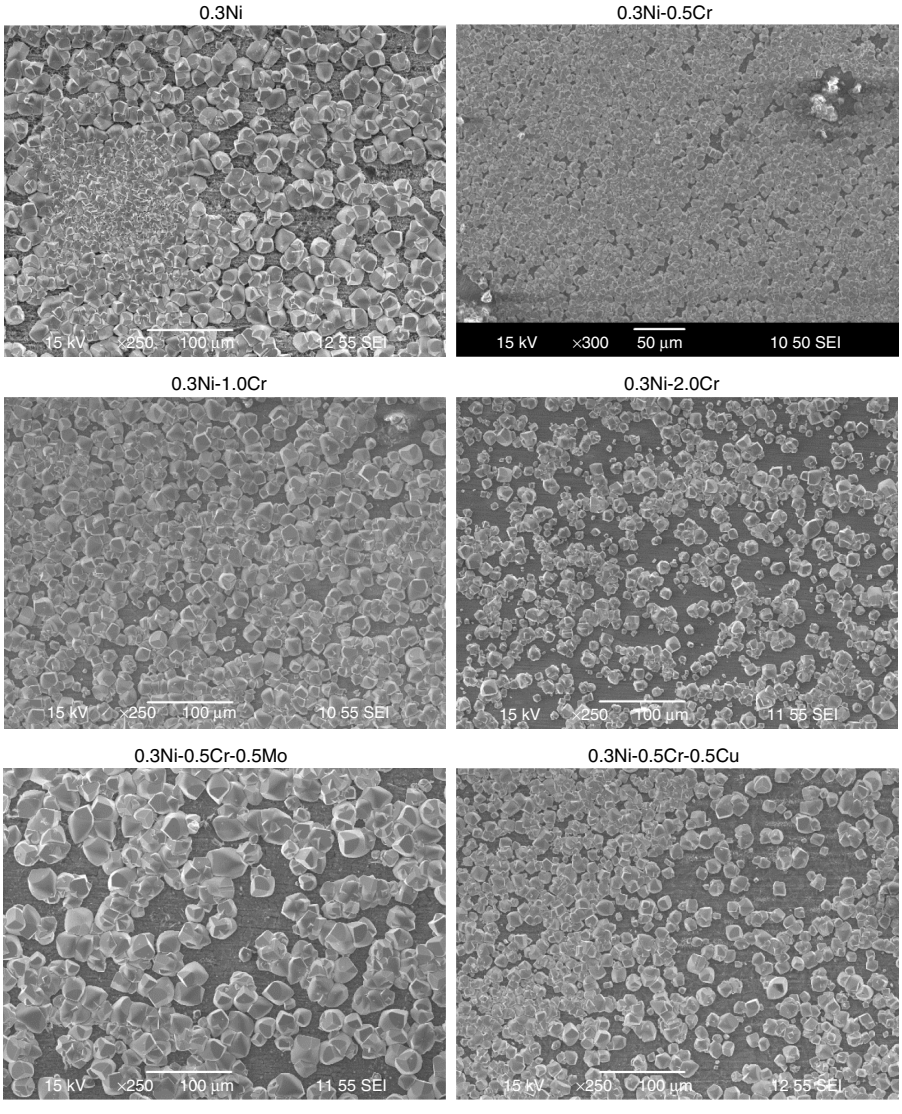

FIGURE 8. *SEM surface images of the corroded samples exposed to 1 wt% NaCl at pH 6.6 and 80°C.*

anodic and cathodic reaction rates were slightly reduced, supporting the decrease in the corrosion rate. Furthermore, slight reduction in anodic and cathodic current densities were also observed by adding Mo and Cu.

Figure 4 shows the variations in corrosion rate and corrosion potential with time for different carbon steels in 1 wt% NaCl at pH 4 and 25°C. 0.3Ni-2.0Cr and 0.3Ni-0.5Cr-0.5Cu steels were selected to conduct long-term corrosion testing because those two steels showed the lowest corrosion rate from the short-term LPR measurement. The corrosion rate and the corrosion potential of 0.3Ni steel increased with time, whereas steels with Cr and Cu showed more or less constant corrosion rate and corrosion potential with time. The fluctuation of corrosion rate was caused by the room temperature change (~10°C) during a day. The corrosion rates of steels with Cr and Cu were slightly lower than that of unalloyed steel, and there is no significant difference in the corrosion rate between 0.3Ni-2.0Cr steel and 0.3Ni-0.5Cr-0.5Cu steel at pH 4 and 25°C.

Figure 5 shows the surface and cross-sectional SEM images of the corroded samples after 7 d in 1 wt% NaCl at pH 4 and 25°C. For all three samples, no corrosion products were observed on the surface because of the test condition (low pH and temperature), and the figure showed mild preferential dissolution of ferrite which left iron carbide (Fe_3C) from the pearlite on the steel.

Experiments at pH 6.6 and 80°C

For these conditions where the formation of protective $FeCO_3$ corrosion product layers was expected, the variations in corrosion rate and corrosion potential with time for different carbon steels in 1 wt% NaCl at pH 6.6 and 80°C are shown in Figures 6 and 7. In contrast to the corrosion behavior at ambient temperature, the corrosion rate of all steel samples decreased with time and reached a low value (<0.1 mm/y) at the end of the experiment. In addition, the corrosion potential of all samples increased when the corrosion rate started to decrease. This indicates that protective $FeCO_3$ layers formed on the steel surface regardless of the alloying elements. The alloying element seemed to affect only the time that it took the corrosion rate to reach the low value.

Figure 8 shows the surface SEM images of the corroded samples at pH 6.6 and 80°C after 3 d. A typical shape of $FeCO_3$ crystals is observed for all samples. There is no correlation between the size of the corrosion product grains and the alloying elements. It is

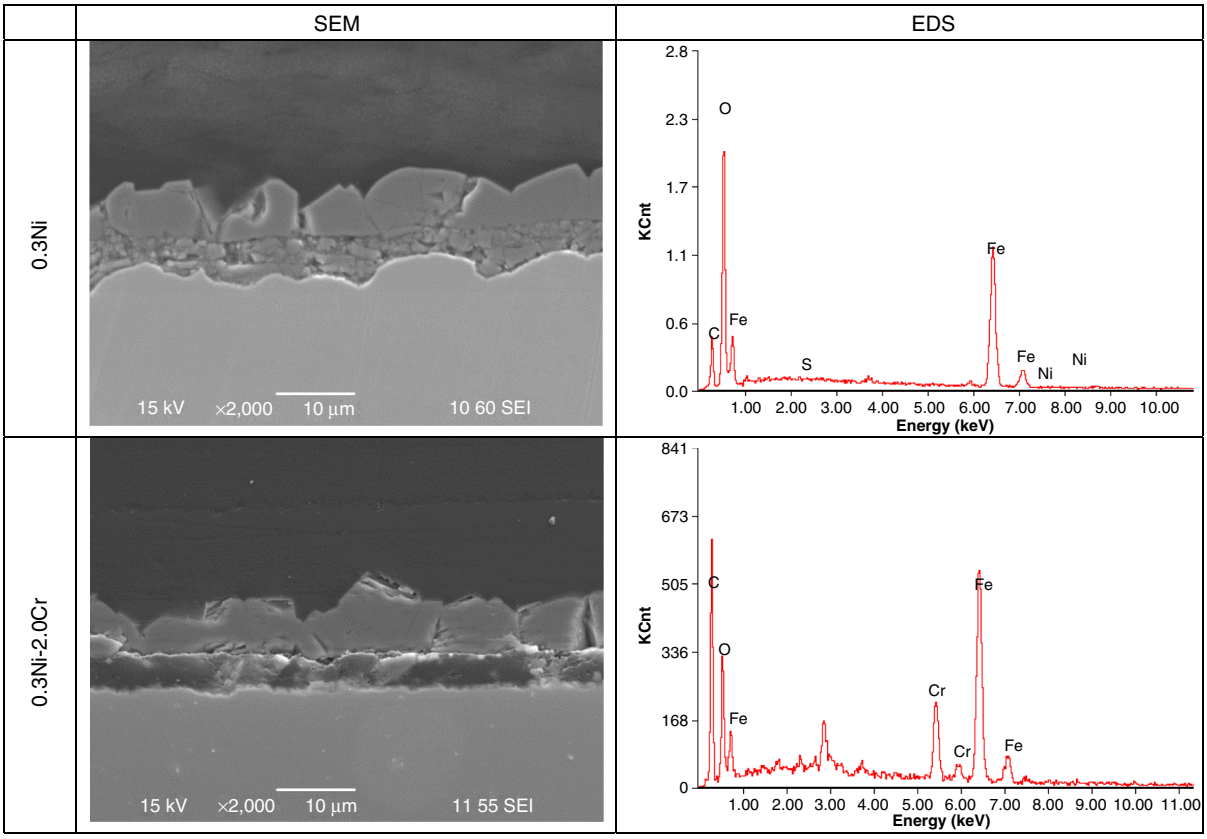

FIGURE 9. *SEM cross-section images and EDS spectra of the inner corrosion product layer exposed to 1 wt% NaCl at pH 6.6 and 80°C.*

interesting to note that for all steel samples, the surface does not appear to be fully covered by corrosion products, even though low and uniform corrosion rates were measured as shown in Figures 6(a) and 7(a). This is because of a much thinner firmly adherent layer underneath that is not readily seen in these images.

Figure 9 represents the cross-sectional morphologies of the samples at pH 6.6 and 80°C after 3 d. It can be seen from all samples that it has a "duplex" layer structure; an outer grainy layer and a continuous adherent inner layer, which seems to be the key to corrosion protection. Similar corrosion product morphologies have been observed recently under different experimental conditions in CO_2 environments.[18] According to EDS results, the outer and inner layers are found to be consistent with $FeCO_3$. The Cr-containing samples showed an enrichment of Cr at the inner layer, while no Cr was detected at the outer crystals. From the cross-sectional observations, it is clear that the corrosion protection is provided by the inner well-attached and dense $FeCO_3$ layer, and not by the outer $FeCO_3$ crystals. Moreover, the alloying elements (Cr, Mo, and Cu) did not contribute to the formation of a more protective $FeCO_3$ layer at pH 6.6 and 80°C.

Experiments at pH 5.9 and 70°C

According to the results shown above, the effect of alloying elements on corrosion behavior was rather small in both the $FeCO_3$-free condition (pH 4, 25°C) and protective $FeCO_3$-forming condition (pH 6.6, 80°C). In other words, the alloying elements do not play a truly significant role either in the undersaturated or supersaturated conditions with respect to $FeCO_3$.

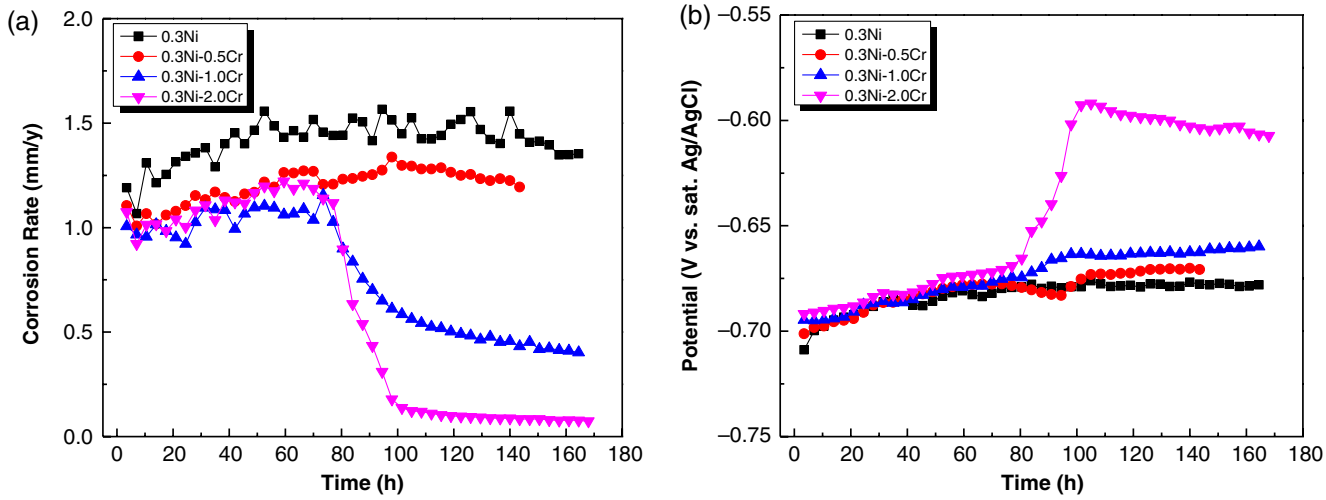

FIGURE 10. *Variations of (a) corrosion rate and (b) corrosion potential for carbon steels with different Cr contents at pH 5.9 and 70°C.*

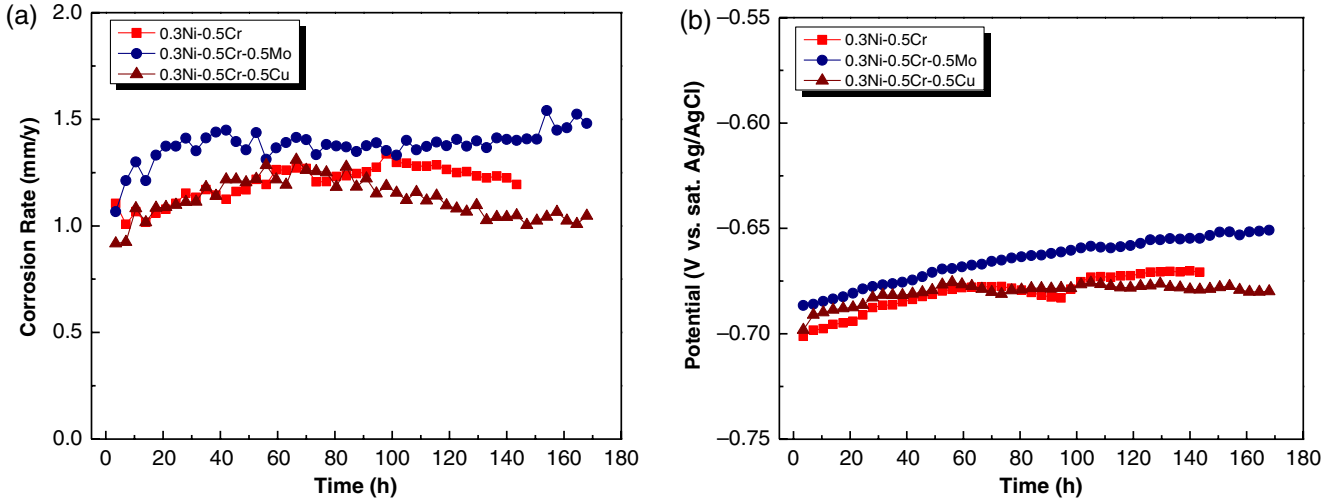

FIGURE 11. *Variations of (a) corrosion rate and (b) corrosion potential for carbon steels with different alloy elements (Mo and Cu) at pH 5.9 and 70°C.*

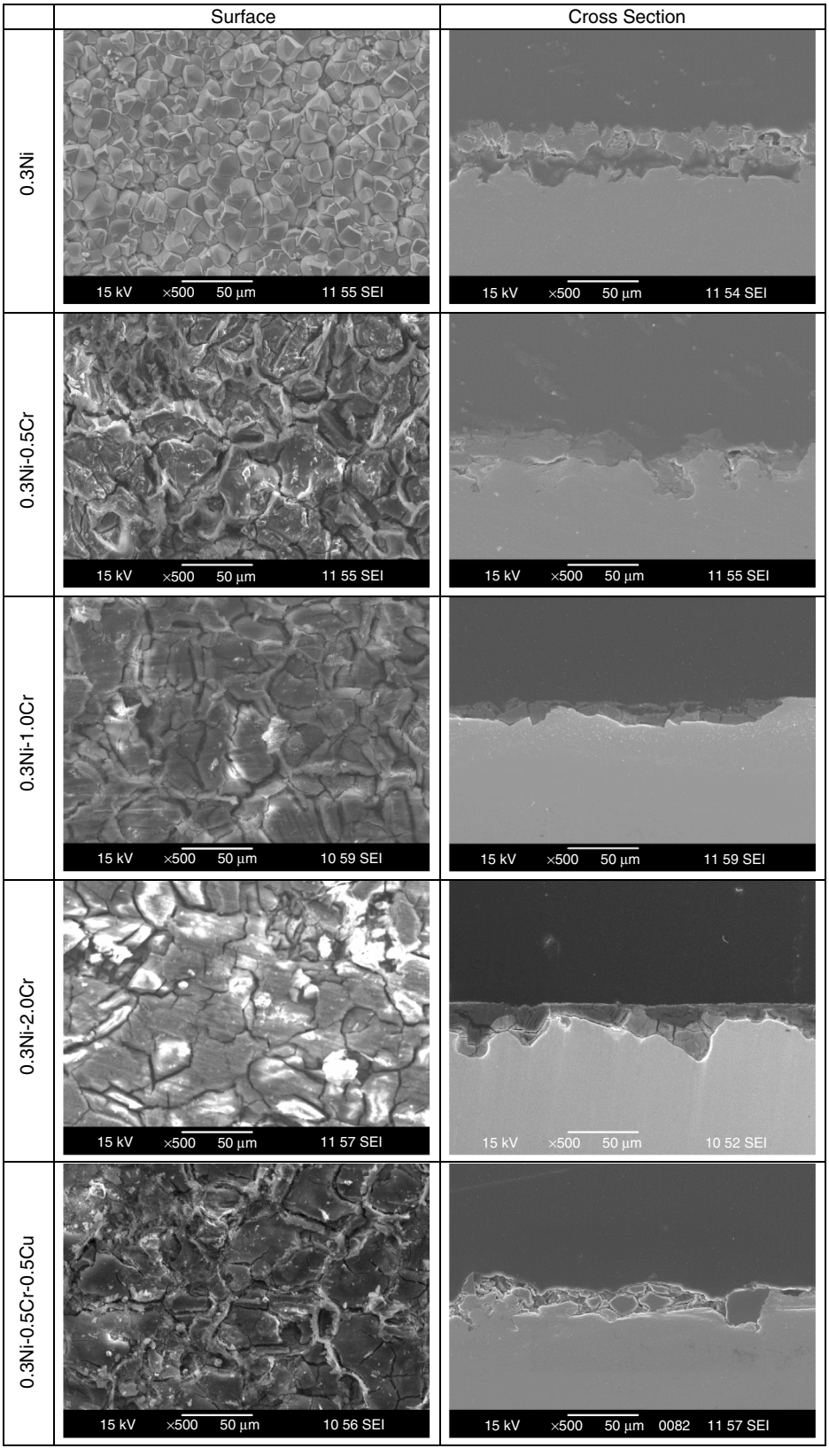

FIGURE 12. *SEM surface and cross-section images of the corroded samples exposed to 1 wt% NaCl at pH 5.9 and 70°C.*

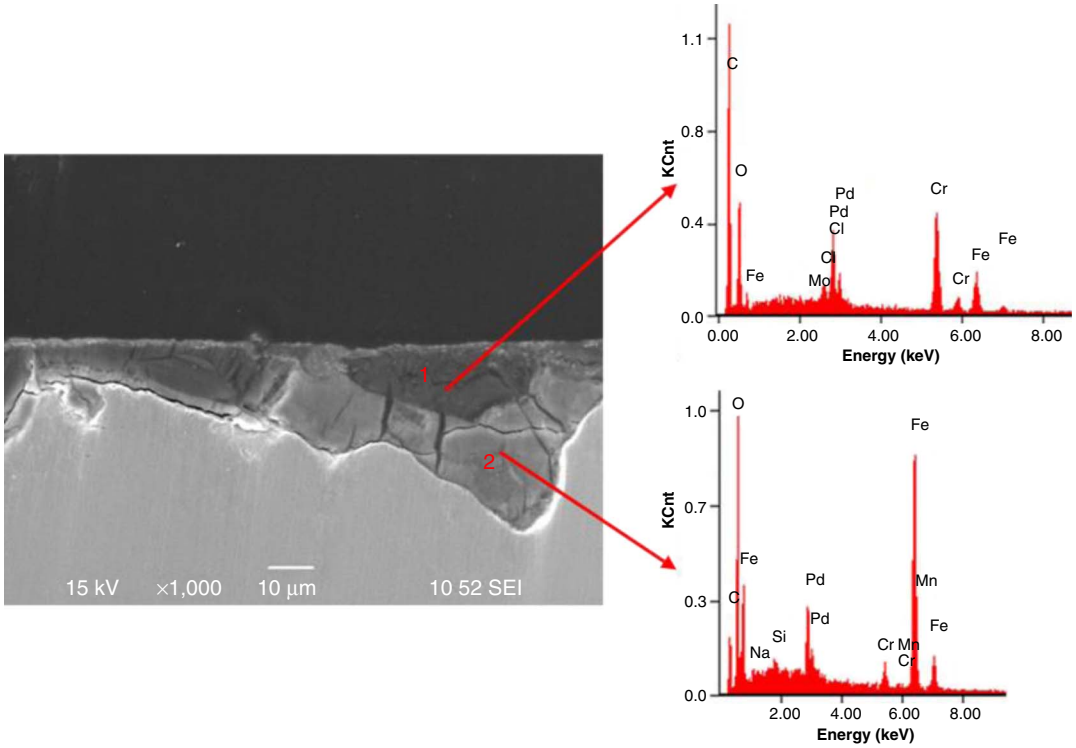

FIGURE 13. *SEM cross-section image and EDS spectra of the corroded sample (0.3Ni-2.0Cr steel) exposed to 1 wt% NaCl at pH 5.9 and 70°C.*

Thus, to further investigate the effect of alloying elements, long-term corrosion tests were conducted in the near-saturated conditions (at pH 5.9, 70°C), where formation of protective $FeCO_3$ is possible but not certain. This intermediate condition is often referred to as the "gray zone."

The variations in corrosion rate and corrosion potential with time for different carbon steels in 1 wt% NaCl at pH 5.9 and 70°C are shown in Figures 10 and 11. It is interesting to observe that the corrosion rate of 0.3Ni-1.0Cr and 0.3Ni-2.0Cr steels decreased with time, whereas other steels showed constant high corrosion rate with time. Only 0.3Ni-2.0Cr steel demonstrated a significant decrease in the corrosion rate with time to truly low values, indicating the formation of fully protective corrosion product layer. It can be clearly seen that with increasing Cr content, the final corrosion rate was decreased, whereas no beneficial effect was observed by adding Mo and Cu under this condition. This suggests that the protectiveness of corrosion product strongly depends on the Cr content of the steel when exposed to solutions in the "gray zone" condition.

Figure 12 shows the surface and cross-sectional SEM images of the corroded samples after 7 d in 1 wt% NaCl at pH 5.9 and 70°C. Although the surface of 0.3Ni steel was fully covered by grainy $FeCO_3$, the corrosion rate was high as shown in Figure 10(a). This can be explained by observing the cross-sectional image, which shows no dense inner layer. The steels containing Cr showed different morphology compared with 0.3Ni steel, i.e., no $FeCO_3$ crystals were observed, but a dense and adherent layer was formed on the steel surface. The layer became denser and more continuous with increasing Cr content, which provided better corrosion protection. It should be mentioned that the presence of Cu showed no beneficial effect on the formation of a protective layer in this condition.

Details of corrosion scale morphology and composition for 0.3Ni-2.0Cr steel were further examined by cross-sectional SEM and EDS, as shown in Figure 13. The layer consists of two distinct areas with respect to Cr content. It is comprised of Cr-rich area with dark contrast and the other area with relatively light contrast, mainly consisting of Fe, C, and O (Table 3). The Pd seen in the EDS spectra is from the sputter coated palladium to avoid any charging during SEM analysis. It has been reported that the presence of Cr results in formation of $Cr(OH)_3$-enriched layer within $FeCO_3$.[13] Furthermore, the presence of Cr^{3+} in the solution has a

TABLE 3

EDS Analysis of 0.3Ni-2.0Cr Steel Exposed to 1 wt% NaCl at pH 5.9 and 70°C

	C (at%)	O (at%)	Cr (at%)	Fe (at%)
1	68.03	13.72	9.66	5.24
2	29.43	26.19	1.88	37.94

significant effect on the precipitation and growth rate of $FeCO_3$.[19-20] Thus, as shown in Figure 13, the beneficial effect of Cr presence in this condition is confirmed by both forming $Cr(OH)_3$ and promoting the formation of thin but adherent and protective $FeCO_3$ layers.

CONCLUSIONS

The effect of alloying elements (Cr, Mo, and Cu) on the corrosion behavior of low carbon steel was investigated in different CO_2 environments. The following conclusions are drawn:

❖ The presence of Cr and Cu showed a slight positive effect on the corrosion resistance at pH 4.0 and 25°C—conditions where protective $FeCO_3$ corrosion product layers do not form.

❖ At pH 6.6 and 80°C, regardless of the alloying elements, the trend of corrosion rate with time was similar, i.e., the corrosion rate of all specimens decreased with time as a result of the formation of protective $FeCO_3$ corrosion product layer.

❖ A beneficial effect of Cr presence was clearly seen at pH 5.9 and 70°C, conditions where protective $FeCO_3$ corrosion product layers could form, but their protectiveness is not certain—in the so-called "gray zone." The steel sample without Cr showed high corrosion rate with time. The presence of Cr promoted the formation of protective $FeCO_3$ layers with Cr enrichment decreasing the corrosion rate significantly.

REFERENCES

1. M. Finšgar, J. Jackson, *Corros. Sci.* 86 (2014): p. 17.
2. Q. Wu, Z. Zhang, X. Dong, J. Yang, *Corros. Sci.* 75 (2013): p. 400.
3. L.G.S. Gray, B.G. Anderson, M.J. Danysh, P.R. Tremaine, "Effect of pH and Temperature on the Mechanism of Carbon Steel Corrosion by Aqueous Carbon Dioxide," CORROSION 1990, paper no. 40 (Houston, TX: NACE International, 1990).
4. C. de Waard, U. Lotz, A. Dugstad, "Influence of Liquid Flow Velocity on CO_2 Corrosion: A Semi-Empirical Model," CORROSION 1995, paper no. 254 (Houston, TX: NACE, 1995).
5. S. Nesic, J. Postlethwaite, S. Olsen, *Corrosion* 52 (1996): p. 280.
6. S. Nesic, *Corros. Sci.* 49 (2007): p. 4308.
7. W. Li, B.F.M. Pots, B. Brown, K.E. Kee, S. Nesic, *Corros. Sci.* 110 (2016): p. 35.
8. D.A. Lopez, T. Perez, S.N. Simison, *Mater. Des.* 24 (2003): p. 561.
9. T. Muraki, T. Hara, K. Nose, H. Asahi, "Effects of Chromium Content up to 5% and Dissolved Oxygen on CO_2 Corrosion," CORROSION 2002, paper no. 272 (Houston, TX: NACE, 2002).
10. L. Xu, B. Wang, J. Zhu, W. Li, Z. Zheng, *Appl. Surf. Sci.* 379 (2016): p. 39.
11. M. Ueda, H. Takabe, "The Formation Behavior of Corrosion Protective Films of Low Cr Bearing Steels in CO_2 Environments," CORROSION 2001, paper no. 066 (Houston, TX: NACE, 2001).
12. S. Guo, L. Xu, L. Zhang, W. Chang, M. Lu, *Corros. Sci.* 63 (2012): p. 246.
13. L. Xu, S. Guo, W. Chang, T. Chen, L. Hu, M. Lu, *Appl. Surf. Sci.* 270 (2013): p. 395.
14. S. Hassani, T.N. Vu, N.R. Rosli, S.N. Esmaeely, Y.S. Choi, D. Young, S. Nesic, *Int. J. Greenhouse Gas Control* 23 (2014): p. 30.
15. J.H. Park, H.S. Seo, K.Y. Kim, S.J. Kim, *J. Electrochem. Soc.* 163 (2016): p. C791.
16. W. Li, L. Xu, L. Qiao, J. Li, *Appl. Surf. Sci.* 425 (2017): p. 32.
17. D.V. Edmonds, R.C. Cochrane, *Mater. Res.* 8 (2005): p. 377.
18. W. Li, B. Brown, D. Young, S. Nesic, *Corrosion* 70 (2014): p. 294.
19. B. Ingham, M. Ko, N. Laycock, N.M. Kirby, D.E. Williams, *Faraday Discuss.* 180 (2015): p. 171.
20. M. Ko, B. Ingham, N. Laycock, D.E. Williams, *Corros. Sci.* 90 (2015): p. 192.